

Time-temperature-transformation (TTT) diagram of a dual-curable off-stoichiometric epoxy-amine system with latent reactivity

Núria [Areny](#)

Osman [Konuray](#)

Xavier [Fernández-Francos*](#)

xavier.fernandez@upc.edu

Josep M. [Salla](#)

Josep M. [Morancho](#)

Xavier [Ramis](#)

Thermodynamics Laboratory, ETSEIB, Universitat Politècnica de Catalunya, Av. Diagonal 647, 08028, Barcelona, Spain

*Corresponding author.

Abstract

The time-temperature-transformation (TTT) diagram of the curing an off-stoichiometric amine-epoxy formulation with intermediate latent reactivity has been elaborated. The first curing stage is an epoxy-amine polycondensation taking place at low temperatures, while the second curing stage is an anionic homopolymerization of the excess epoxy groups, taking place at high temperatures and catalyzed by a latent base. The curing kinetics of the first and second curing stages have been analyzed separately by integral isoconversional procedures, and the kinetics data has been used to plot the isoconversion lines in the TTT diagram. The relationship between the glass transition temperature (T_g) and conversion has been determined experimentally and theoretically and used to determine the vitrification line in the TTT diagram. The results reflect the clearly different kinetic behaviour of both curing stages and a significant intermediate storage stability, which makes these curing systems highly attractive for multiple stage processing. The shape of the vitrification line also reflects the occurrence of different curing processes with different structure build-up. Safe processing and storage conditions can be easily defined on the basis of the TTT diagram. This is the first time the curing behavior of dual-curing formulations is illustrated in such a clear and concise way thanks to the TTT diagram.

Keywords: Epoxy; [Diamine](#); [Dual-Curing](#); [Latent base](#); [Thermosets](#); [Time-Temperature-Transformation \(TTT\) diagram](#)

1 Introduction

Dual-curing, that is, the combination of two different polymerization processes taking place simultaneously or sequentially in a curing process, is a highly advantageous technology for the processing of thermosetting systems [1,2] because of its versatility and flexibility. A significant added value of sequential dual curing is possibility of controlling the curing process sequence and the intermediate and final network structures and properties [3-5]. This has potential application in multi-stage processing of one-pot formulations, where materials can be partially pre-cured before their storage, and with tailored material properties for the final application [4-7]. Processing or assembly and the final properties can be achieved whenever desired by using heat or UV light, depending on formulation chemistry, to initiate the final curing stage. Click-type reactions are commonly used in dual-curing formulations [1], in combination with other click [8,9] or non-click reactions [3,5]. Many dual-curable systems are based on acrylate reactions [2,5], although systems based on epoxy curing chemistries such as off-stoichiometric thiol-epoxy [3] or epoxy-amine [4,10] formulations, or other epoxy systems [11], are also gaining interest in the recent years.

We recently developed a novel off-stoichiometric epoxy-amine system, with excess epoxy groups and latent reactivity in the intermediate state [4]. The first curing reaction was a self-limiting epoxy-amine condensation that takes place at moderate temperatures until exhaustion of reactive amine groups. In the presence of a suitable initiator such as a nucleophilic tertiary amine [10], the excess of epoxy groups can undergo anionic homopolymerization at higher temperatures. However, in this recent work we employed a latent thermal base for the epoxy homopolymerization [4], which ensured at least 7 weeks of storage stability at 30 °C for intermediate materials after the completion of the epoxy-amine reaction. Different materials, coming from a wide range of formulations with different amine-epoxy ratios and tailored intermediate and final properties, were analyzed and characterized, but the curing kinetics of

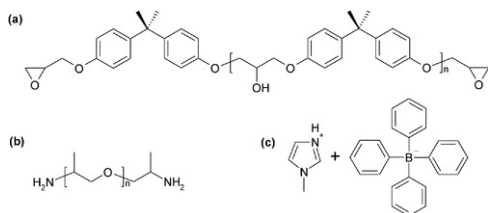
the systems were not analyzed in detail.

The purpose of this paper is to study the curing kinetics of an off-stoichiometric epoxy-amine formulation with a latent thermal base for the activation of the homopolymerization of the epoxy groups in excess. The relationship between glass-transition (T_g) and degree of conversion x is also determined (i.e. the $T_g(x)$ relationship). Gelation is not analyzed but the results from a previous work are used [4]. The results of this analysis are summarized in the conversion-temperature-transformation (CTT) diagram [12] and the time-temperature-transformation (TTT) diagram [13-16], which are used to illustrate the main transformations taking place during curing (i.e. gelation and vitrification) and the particular features of this dual-curing system. The CTT and TTT diagrams are also used to illustrate the predictive capabilities of the kinetic modelling employed in this work. The curing kinetics and glass transition temperatures are analyzed using differential scanning calorimetry (DSC). Isoconversional procedures are employed to determine the kinetic parameters, plot the isoconversional and vitrification lines of the TTT diagram and simulate other curing programmes.

2 Experimental

2.1 Materials

Diglycidyl ether of bisphenol A (DGEBA, $M_w = 374$ g/mol or $M_w = 187$ g/ee, EpikoteTM) (DG hereafter) was kindly supplied by Hexion speciality Chemical B.V. and dried in vacuum before use. All other chemicals and reagents were purchased from Sigma-Aldrich and used as received. Poly(propylene glycol) bis(2-aminopropyl ether) (Jeffamine, $M_w = 400$ g/mol) (JEF hereafter), 1-methylimidazole (1MI) and sodium tetraphenylborate (NaBPh₄) were supplied by Aldrich and used as received. Methanol (MeOH) and chloroform (CHCl₃) were supplied by VWR and were used as received. 1MI-HBPh₄ (BG hereafter) was prepared using the procedure outlined in the literature [17,18]. Firstly, 1MI was solubilized in H₂O slightly acidified with 36% HCl solution (10 mmol in 2.6 mL H₂O and 1 mL HCl). NaBPh₄ was also solubilized in H₂O (11 mmol in 10 mL H₂O) stirred until homogeneous. The two solutions were mixed and the stirring maintained until the white salt formed as precipitate. The salt was filtered, washed thoroughly with distilled water and MeOH, recrystallized from a 4:1 mixture of MeOH and CHCl₃, filtered and dried under mild heat and vacuum. To analyze its purity, its melting point was measured in a DSC thermal scan and was found to be similar to what is reported for other equivalent salts [17,18]. The structures of DG, JEF, and BG are shown in Scheme 1.



Scheme 1 : Molecular structures of the chemicals used: (a) DGEBA (DG), (b) Jeffamine (JEF) and (c) 1MI-HBPh₄ (BG).

alt-text: Scheme 1

2.2 Preparation of the curing mixtures

Samples were prepared in 5 mL vials in 1-2 gr batches using the following procedure: BG was weighed and added to DG and was kept under agitation at 90 °C for 15 min at complete solubilization. The mixture was left to cool down to room temperature after which the required amount of JEF was added, quickly stirred and immediately sent to analysis or sample preparation. DGJEF_0.5_BG4 is a formulation in which one half of epoxy equivalents react with amine hydrogens and the other half homopolymerizes in the second curing stage, and 4 wt.% of BG. DGJEF_0.5 is the epoxy-amine formulation with the same excess of epoxy groups but without added initiator. DG_BG4 is the neat DG formulation with 4 wt.% of BG. The details of the composition of the formulations are shown in Table 1.

Table 1 - Notation and composition of the formulations studied in this work.

alt-text: Table 1

Formulation	r^a	DG (wt. %)	JEF (wt. %)	BG (wt. %)	eq_{BG}/ee^b
DGJEF_0.5	0.5	78.9	21.1	0	0
DGJEF_0.5_BG4	0.5	75.7	20.3	4	0.0245
DG_BG4	0	96	0	4	0.0194

^a Ratio between reactive amine hydrogens and epoxy groups.

^b Equivalents of 1MI/Equivalents of epoxy groups.

2.3 Experimental techniques

A Mettler DSC822e equipped with a robotic arm was used. The equipment was calibrated using indium standards. Approximately 10 mg samples were cured in aluminium pans with pierced lids under a nitrogen atmosphere. The DSC was used to study the nonisothermal curing at 10 °C/min up to 300 °C and the isothermal curing at temperatures in the range of 70–100 °C for the first curing process, and 160–190 °C for the second curing process after pre-curing of the samples at 90 °C for 240 minutes. The degree of cure of the epoxy groups, x , and the reaction rate, dx/dt , were calculated as follows:

$$x = \frac{\Delta h_T}{\Delta h_{total}} \quad x = \frac{\Delta h_t}{\Delta h_{total}} \quad \text{(There are two expressions, } x=\Delta h_T/\Delta h_{total} \text{ and } x=\Delta h_t/\Delta h_{total}, \text{ check the spacing. I could not correct it with the math editor. Please verify the submitted manuscript.)} \quad (1)$$

$$\frac{dx}{dt} = \frac{dh/dt}{\Delta h_{total}} \quad (2)$$

where Δh_T and Δh_t are the heat evolved up to a temperature T or time t during a dynamic or isothermal curing experiment, respectively. Δh_{total} is the total heat released during curing and dh/dt is the instantaneous heat flow released.

The glass transition temperature of the uncured formulation T_{g0} was determined in the dynamic curing at 10 °C/min starting at -100 °C. The intermediate glass transition temperature (T_{gint}) of the dual DGJEF_0.5_BG4 was determined in a dynamic scan at 10 °C/min after isothermal curing at 90 °C for 240 minutes. The ultimate glass transition temperature ($T_{g\infty}$) of the fully cured sample (at 180 °C for enough time so as to complete the curing process) was determined after two consecutive dynamic scans at 10 °C/min, the first one to determine the presence of residual heat. The T_g was determined as the midpoint in the heat capacity step during the glass transition. The increase in heat capacity during the glass transition, ΔC_p , was also determined. The DIN method, included in the STARE software by Mettler, was used for these determinations.

The relationship between the degree of conversion and the glass transition temperature, $T_{g(x)}$, was determined from partially cured samples that were subsequently heated up at 10 °C/min to determine their T_g and the residual heat Δh_{res} , which allowed to determine the degree of conversion as:

$$x = 1 - \frac{\Delta h_{res}}{\Delta h_{total}} \quad (3)$$

3 Theoretical

3.1 Curing kinetics

The isoconversional methodology was used for the determination of the apparent activation energy during the curing process [19]. The basis for this methodology is the assumption that the reaction rate can be expressed as separate functions of conversion x and temperature T as:

$$x = 1 - \frac{\Delta h_{res}}{\Delta h_{total}} \quad \frac{dx}{dt} = k(T) \cdot f(x) \quad \text{(The whole equation was wrong. Please check the original manuscript. it should be } dx/dt=k(T) \cdot f(x). \text{ I have already corrected it.)} \quad (4)$$

Where $k(T) = A \exp(-E/RT)$ is the kinetic constant, A is the preexponential factor, E is the activation energy, R is the gas constant and $f(x)$ is the model representing the reaction mechanism governing the curing process. In other words, it is assumed that the reaction mechanism is not affected by the temperature schedule of the curing process. Therefore, the apparent activation energy at a given degree of conversion E_x can be calculated as follows:

$$x = 1 - \frac{\Delta h_{res}}{\Delta h_{total}} \quad \frac{d \ln(dx/dt)}{dT^{-1}} = \frac{d \ln(f(x))}{dT^{-1}} + \frac{d \ln(k(T))}{dT^{-1}} \equiv -\frac{E_x}{R} \quad \frac{d \ln(dx/dt)}{dT^{-1}} = \frac{d \ln(f(x))}{dT^{-1}} + \frac{d \ln(k(T))}{dT^{-1}} \equiv -\frac{E_x}{R} \quad (5) \quad \text{(The equation was wrong. The beginning of it, } x=1-\Delta h_{res}/\Delta h_{total}, \text{ had to be removed. I have corrected it, please check the submitted manuscript.)}$$

This is the basis for the differential or Friedman method. Linear regression of $\ln(dx/dt)$ against the inverse of temperature for different experiments at a given degree of conversion, yields the slope $-E_x/R$ and the intercept at the origin $\ln(A_x f(x))$.

Rearrangement and integration of the rate expression leads to:

$$g(x) = \int_0^x \frac{dx}{f(x)} = A \cdot \int_0^t \exp(-E/R \cdot T) \cdot dt \quad (6)$$

Under isothermal conditions, this leads to the following expression, taking natural logarithms:

$$\ln t = \ln \left(\frac{g(x)}{A} \right) + \frac{E}{R \cdot T} \quad (7)$$

Representation of $\ln t$ against $(R \cdot T)^{-1}$ for different experiments at a given degree of conversion yields a straight line with slope E_x and intercept at the origin $\ln(g(x)/A_x)$. Note that these kinetic parameters are not equivalent to those determined using the differential method [19,20] and should not be exchanged unless the value of the differential apparent isoconversional energy, E_x , remains constant throughout the curing process. Other expressions can be found for non-isothermal curing processes [21-23]. In the case of dynamic curing experiments, one has to resort to the original integral expression Eq. (6). Under constant heating rate conditions, the integral expression can be rewritten as:

$$\frac{g(x)}{A} = \frac{1}{\beta} \cdot \int_0^T \exp(-E/R \cdot T) \cdot dT = \frac{1}{\beta} \cdot \frac{E}{R} \cdot p(y) \quad (8)$$

Where β is the heating rate, $y = E/RT$ and $p(y)$ is an approximation of the solution of the temperature integral, making use of the more exact approximations such as the ones of Senum and Yang [22]. The determination of parameters $\ln(g(x)/A_x)$ and E_x may require numerical iteration procedures [24], but some approximations of $p(y)$ make it possible to derive linear isoconversional methods [21]. In the present case, however, the kinetic parameters will only be determined from isothermal experiments.

In sequential dual-curing processes, the curing kinetics of the process can be analyzed from a global point of view [3] or individually [11]. Simulations can be performed by sequential integration of rate expressions [3,11], which can be a reasonable assumption depending on the chemistry behind the dual-curing process [3,25]. Note that this is inherent in the application of isoconversional analysis to complex multi-step processes, which can be safely analyzed using isoconversional methods providing the coexisting processes are not competitive [26] but sequential [19], as in some dual-curing systems [3].

However, it may be that the curing process is not strictly sequential depending on the temperature programme, that is, that the activation of the second curing process is somewhat independent from the completion of the first curing process, leading to overlapping of the curing processes under certain temperature programmes [11]. In the present case, we choose to analyze the curing processes independently, and we also assume that the activation of both curing process is independent as well, that is, the second curing process is not activated immediately after the end of the first one but has its own activation kinetics (i.e. slow thermal decomposition of BG leading to the release of the initiator). The methodology we follow is different from that of the work of Sun et al. [11], which analyzed the curing kinetics of a dual system under non-isothermal conditions. In this case, the first curing process is analyzed under isothermal conditions at which the second curing process is not yet activated; the second curing process is analyzed at high temperatures after precuring of the samples at 90 °C for 240 min. This precuring is necessary in order to complete the first curing process but avoiding premature activation of the second one.

The individual kinetics analysis of the first curing process would not be affected. Therefore, Eq. (7) is used for the determination of the kinetic parameters $\ln(g_1(x_1)/A_{1,x})$ and $E_{1,x}$ for a given degree of conversion x_1 . Eq. (7) is also used for the isothermal simulation at other temperatures.

In the case of the second curing process, the thermal history should be taken into consideration in the analysis. The kinetics analysis of the second curing process should start from the general integral expression, Eq. (6). Taking into account the presence of this preliminary thermal programme, one could write for the second curing process:

$$g_2(x) = A_2 \cdot \int_0^{t_1} \exp(-E_2/R \cdot T_1) \cdot dt + A_2 \cdot \int_{t_1}^{t_1+t_2} \exp(-E_2/R \cdot T_2) \cdot dt \quad (9)$$

Where t_1 is the time at the end of the first thermal programme, and t_2 is the experimental reaction time of the second curing process, which is analyzed independently. The value of the total onset time for the analysis of the second curing process would be $t_1 + t_2$. T_1 and T_2 are the temperature programmes of the first and second curing process (up to the reaction onset in this case). Note that the value of preexponential factor A_2 and activation energy E_2 should be identical in both integrals, because they correspond to the second curing process.

If one calls $I_1 = \int_0^{t_1} \exp(-E_2/R \cdot T_1) \cdot dt$, and the second curing process is analyzed under isothermal conditions, then:

$$\frac{g_2(x)}{A_2} = I_1 + \exp(-E_2/R \cdot T_2) \cdot t_2 \quad (10)$$

Taking natural logarithms:

$$\ln t_2 = \ln \left(\frac{g_2(x)}{A_2} - I_1 \right) + \frac{E_2}{R \cdot T_2} = C + \frac{E_2}{R \cdot T_2} \quad (11)$$

Representation of $\ln t_2$ against $(R \cdot T_2)^{-1}$ for different experiments at a given degree of conversion x yields a straight line with slope $E_{2,x}$ and intercept at the origin $C_x = \ln(g_2(x_2)/A_{2,x} - I_1)$. The value of I_1 is calculated making use of $E_{2,x}$ but taking into consideration the value of T_1 corresponding to the first curing process. For an isothermal precuring stage at T_1 , this is simply $I_1 = \exp(-E_{2,x}/R \cdot T_1) \cdot t_1$. The value of $\ln(g_2(x_2)/A_{2,x})$ can therefore be determined as:

$$\ln \left(\frac{g_2(x_2)}{A_{2,x}} \right) = \ln (e^{C_x} + I_1) \quad (12)$$

This procedure based on the linear regression is only strictly possible in the case that all the samples have been pre-cured under the same conditions, that is, the value of I_1 is equal for all the experiments. If not, a non-linear fitting of $\ln(g_2(x_2)/A_{2,x})$ and $E_{2,x}$ would be necessary.

Note that, in this analysis, the value of $E_{2,x}$ does not depend on the inclusion of the I_1 term, as in a conventional isoconversional analysis. Instead, it affects only the value of $\ln(g_2(x_2)/A_{2,x})$. The values of $\ln(g_2(x_2)/A_{2,x})$ and $E_{2,x}$ could be used in Eq. (7) to easily predict curing times of the second curing process, assuming the whole process takes place under isothermal conditions, as in the TTT diagram.

This approach could be generalized for the analysis of kinetics data from non-isothermal curing programmes or combinations of isothermal and non-isothermal data, although this could involve numerical integration or the use of numerical approximations (i.e. for constant heating rate experiments) and numerical fitting instead of simple linear regression methods.

3.2 T_g - x relationship

In order to model the dependence of the T_g on the degree of conversion $T_{g(x)}$, the expression derived by Venditti and Gillham [27] has been used:

$$\ln T_g(x) = \frac{(1-x) \cdot \ln T_{g0} + \lambda \cdot x \cdot \ln T_{g\infty}}{(1-x) + \lambda \cdot x} \quad (13)$$

$$\lambda = \frac{\Delta C_{p\infty}}{\Delta C_{p0}} \quad (14)$$

where $T_{g\infty}$ and T_{g0} are the glass transition temperatures of the crosslinked and uncured materials, respectively, and $\Delta C_{p\infty}$ and ΔC_{p0} are the increase in heat capacity during the glass transition of the crosslinked network and the uncured material. All these parameters are determined from only two experiments carried out with DSC, a dynamic scan at 10 °C/min of the uncured and fully cured samples, thus saving a significant amount of experimental time. There are other expressions such as the one derived by Pascault and Williams [12,28] that provide comparable results. The parameter λ can also be determined from an experimental $T_{g(x)}$ relationship determined as described in the experimental section.

In the present case, a single $T_{g(x)}$ relationship, making use of expression (13), cannot be determined, because the curing takes place in two different curing stages involving different clearly different curing reactions with different molecular growth and network build-up mechanisms. Given that T_g is highly dependent on the evolution of molecular weight/structure and network architecture [29], a separate analysis should be carried out for both curing stages. Therefore, expression (13) should be applied to the first part of the curing process in order to determine $T_{g,1(x)}$ (making use of T_{g0} , T_{gint} and $\lambda = \Delta C_{pint}/\Delta C_{p0}$) and to the second part of the curing process in order to determine $T_{g,2(x)}$ (making use of T_{gint} , $T_{g\infty}$ and $\lambda = \Delta C_{p\infty}/\Delta C_{pint}$). T_{gint} and ΔC_{pint} are determined from the analysis of the intermediate material, after completion of the first curing stage. This is the end point of the first curing process, and the starting point of the second curing process.

3.3 Time-temperature-transformation (TTT) diagram

The results of the study of the curing process are used to build the conversion-temperature-transformation (CTT) and time-temperature-transformation (TTT) diagrams [12-16] summarizing the most relevant transformations taking place during processing and the kinetics of the curing process. Different states are also usually represented: (1) soluble glass, below T_{g0} and at any $T < T_{g(x)}$ and $x < x_{gel}$, (2) liquid, at any $T > T_{g(x)}$ and $x < x_{gel}$, (3) gelled glass for any $T < T_{g(x)}$ and $x > x_{gel}$, and (4) gelled rubber for any $T > T_{g(x)}$ and $x > x_{gel}$. In the CTT diagram, the vitrification line $T_{g(x)}$ and gelation line x_{gel} are represented, and in addition to other lines representing curing processes can be represented. In the TTT diagram, the time is explicitly taken into account, so that different lines have to be represented: (1) isoconversional lines representing the time needed to reach a certain degree of conversion, isothermally, at

different temperatures, (2) the gelation line, considered isoconversional and (3) the vitrification line, representing the time needed to reach $T = T_g$, which is not isoconversional. Degradation at higher temperatures leading to char or devitrification can also be represented [30]. All this information may be necessary in order to define safe and time/cost-effective curing schedules reaching the desired ultimate properties, or to outline multiple-stage curing processes [31].

The particular features of sequential dual-curing processes, combining polymerization processes with different reactivity [3,4], however, may produce a TTT diagram with some enhanced features. Isoconversional lines describing the curing kinetics both curing processes should be included, and a vitrification line for each process should be represented as well.

For the isoconversional lines corresponding to the first curing processes, the isoconversional integral parameters were obtained from the analysis of the isothermal curing experiments using Eq. (7) and the time needed to reach a given conversion x was calculated using Eq. (7). Isoconversional lines were represented starting from $T = T_{g,1}(x_1)$ (the $T_{g(x)}$ relationship of the first curing process) up to 200 °C.

In the case of the second curing processes, the isoconversional integral parameters were obtained from the analysis of the isothermal curing experiments using eEq. (11), and the time needed to reach a given conversion x was calculated using Eq. (7). Isoconversional lines were represented starting from $T = T_{g,2}(x_2)$ (the $T_{g(x)}$ relationship of the second curing process) up to 200 °C.

Note that, given the composition of the DGJEF_0.5_BG4 formulation (see Table 1), a global conversion of epoxy groups can be defined as:

$$x_{epoxy} = 0.5 \cdot x_1 + 0.5 \cdot x_2 \quad (15)$$

Therefore, for the sake of simplicity, in the diagram we have represented the global isoconversional lines (x_{epoxy}). Assuming that the first process is complete before the second process is started, we calculated $x_{epoxy} = 0.5 \cdot x_1$ for the first curing process, and $x_{epoxy} = 0.5 + 0.5 \cdot x_2$ for the second curing process.

Unlike other works [14,31], the effect of vitrification on curing kinetics was not modelled nor included in the calculation of the TTT diagram, because the curing processes were always analyzed at temperatures sufficiently above $T_{g(x)}$. The vitrification lines were finally determined joining the end points of the isoconversional lines.

3.4 Simulation and prediction of curing schedules

Strictly isothermal curing schedules can be easily simulated or determined from the TTT diagram, because they are horizontal lines at the prescribed temperatures. Different curing schedules, other than merely isothermal curing processes, can be simulated. Some complex scenarios, combining different isothermal and dynamic curing stages, are explained in detail in the following paragraphs. For more complex processes in which isothermal or constant heating rate conditions cannot be guaranteed, such as the curing of composite parts with accumulation of heat and likely occurrence of temperature overshoots, other methods, based on the numerical integration of rate equations and energy balances should be applied [12,32].

3.4.1 Dynamic curing at constant heating rate

Once the parameters $\ln(g(x)/A_x)$ and E_x have been determined from an integral isoconversional analysis for a given degree of conversion x , the temperature T_x at which x is reached in an experiment with constant heating rate β is determined by numerical iteration until both sides of Eq. (8) reach the same value. In this work, we have chosen to use the 4th order approximation of Senum and Yang [22]. In the case of the dual-curing process under study, this calculation should be made for each one of the curing processes independently, and referred to the global conversion x_{epoxy} assuming that $x_{epoxy} = 0.5 \cdot x_1$ for the first curing process, and $x_{epoxy} = 0.5 + 0.5 \cdot x_2$ for the second curing process. This leads to a $T_x - x$ curve that can be easily represented in a conversion-time-temperature (CTT) diagram [12]. Representation of the $T_x - x$ curve in the TTT diagram would imply the transformation of temperature into equivalent isothermal time making use Eq. (7), but this has not been performed in order to avoid confusions.

3.4.2 Two consecutive isothermal stages

Another possible scenario to be analyzed is a two-stage curing process in which the material is first pre-cured at an isothermal temperature to complete the first curing process, and then the system is heated up at another temperature to complete the second curing process. This is the inverse problem to that of the isoconversional analysis methodology described before. In this case, it has some interest to calculate or determine the required isothermal time of the second stage to complete the second curing process after the first pre-curing. Estimation of this second time, t_{stage2} , is simply performed by the use of Eq. (11) for a degree of conversion close to complete curing, with given values of $E_{2,x}$ and $\ln(g_2(x)/A_{2,x})$, and second stage temperature T_2 . According to Eq. (11), it is necessary to first calculate the value of I_1 corresponding to the first precuring stage. Under isothermal conditions, with temperature T_1 and a time t_{stage1} , is simply $I_1 = \exp(-E_{2,x}/R T_1) \cdot t_{stage1}$. Finally, the total cycle time is determined as $t_{cycle} = t_{stage1} + t_{stage2}$.

3.4.3 Two consecutive isothermal stages with heating ramps

The calculations become somewhat more complex if one takes into account the heating ramp needed to first raise the temperature to T_1 with a heating rate β_1 , the isothermal step at T_1 to complete the first curing process, and the ramp needed to then raise the temperature to T_2 with a heating rate β_2 .

If one wants to determine, first of all, the time needed in the first isothermal step at T_1 , $t_{1,iso1}$, to complete the first curing reaction, one can write, starting from Eqs. (6) or (11):

$$t_{1,iso1} = \left(\frac{g_1(x)}{A_{1,x}} - I_{1,dyn1} \right) \cdot \exp\left(\frac{E_{1,x}}{R \cdot T_1} \right) \quad (16)$$

Where $g_1(x)/A_{1,x}$ and $E_{1,x}$ are the integral isoconversional parameters corresponding to a degree of conversion close to the completion of the first curing process, and $I_{1,dyn1}$ is the contribution of the dynamic heating step to the time/temperature integral (Eq. (6)). $I_{1,dyn1}$ can be calculated, starting from Eq. (8), as

$$I_{1,dyn1} = \frac{1}{\beta_1} \cdot \int_{T_0}^{T_1} \exp(-E_{1,x}/R \cdot T) \cdot dT = \frac{1}{\beta_1} \cdot \frac{E_{1,x}}{R} \cdot \left[p(y_{1,T_1}) - p(y_{1,T_0}) \right] \quad (17)$$

$$y_{1,T_1} = \frac{\int_{T_0}^{T_1} \exp(-E_{1,x}/R \cdot T) \cdot dT}{R \cdot T_1} \quad y_{1,T_0} = \frac{\int_{T_0}^{T_0} \exp(-E_{1,x}/R \cdot T) \cdot dT}{R \cdot T_0} \quad \text{(Please note that there are two expressions that are separated, one is } y_{1,T_1} = E_{1,x}/(R \cdot T_1), \text{ and the other is } y_{1,T_0} = E_{1,x}/(R \cdot T_0). \text{ There should be a spacing between them. Apparently there is a spacing if I open it with the math editor. Please verify the submitted manuscript.)}$$

, making use of the 4th order approximation of Senum and Yang [22] for the temperature integral, $p(y)$. Note that the value of $p(y_{1,T_0})$ corresponds to the beginning of the heating process, but its value can be negligible, as in the definition of dynamic integral methods. Once this is done, the total time of the first curing stage (heating + isothermal at T_1 is calculated as:

$$t_{stage1} = \frac{T_1 - T_0}{\beta_1} + t_{1,iso1} \quad (18)$$

In the case of the second curing stage, one might be interested in calculating the time needed in the second isothermal step at T_2 , $t_{2,iso2}$, to complete the second curing reaction, taking into account all the previous thermal history (recall that the kinetics of second curing stage are modelled as an event independent from the first curing stage):

$$t_{2,iso2} = \left(\frac{g_2(x)}{A_{2,x}} - I_{2,dyn1} - I_{2,iso1} - I_{2,dyn2} \right) \cdot \exp\left(\frac{E_{2,x}}{R \cdot T_2} \right) \quad (19)$$

Where $g_2(x)/A_{2,x}$ and $E_{2,x}$ are the integral isoconversional parameters corresponding to a degree of conversion close to the completion of the second curing process. $I_{2,dyn1}$, $I_{2,iso1}$ and $I_{2,dyn2}$ are the contributions of the first dynamic, first isothermal and second dynamic steps, respectively, to the time/temperature integral (Eq. (6)). They can be calculated using the following set of expressions:

$$I_{2,dyn1} = \frac{1}{\beta_1} \cdot \int_{T_0}^{T_1} \exp(-E_{2,x}/R \cdot T) \cdot dT = \frac{1}{\beta_1} \cdot \frac{E_{2,x}}{R} \cdot \left[p(y_{2,T_1}) - p(y_{2,T_0}) \right] \quad (20)$$

$$y_{2,T_1} = \frac{\int_{T_0}^{T_1} \exp(-E_{2,x}/R \cdot T) \cdot dT}{R \cdot T_1} \quad y_{2,iso1} = \frac{\int_{T_1}^{T_1} \exp(-E_{2,x}/R \cdot T) \cdot dT}{R \cdot T_1} \quad y_{2,T_0} = \frac{\int_{T_0}^{T_0} \exp(-E_{2,x}/R \cdot T) \cdot dT}{R \cdot T_0} \quad \text{(Please note that there are two expressions that are separated, one is } y_{2,T_1} = E_{2,x}/(R \cdot T_1), \text{ and the other is } y_{2,T_0} = E_{2,x}/(R \cdot T_0). \text{ There should be a spacing between them. Please verify the submitted manuscript.)}$$

$$I_{2,iso1} = \exp(-E_{2,x}/R \cdot T_1) \cdot t_{1,iso1} \quad (21)$$

$$I_{2,dyn2} = \frac{1}{\beta_2} \cdot \int_{T_1}^{T_2} \exp(-E_{2,x}/R \cdot T) \cdot dT = \frac{1}{\beta_2} \cdot \frac{E_{2,x}}{R} \cdot \left[p(y_{2,T_2}) - p(y_{2,T_1}) \right] \quad (22)$$

$$y_{2,T_2} = \frac{\int_{T_0}^{T_2} \exp(-E_{2,x}/R \cdot T) \cdot dT}{R \cdot T_2} \quad y_{2,T_1} = \frac{\int_{T_0}^{T_1} \exp(-E_{2,x}/R \cdot T) \cdot dT}{R \cdot T_1} \quad \text{(Please note that there are two expressions that are separated, one is } y_{2,T_2} = E_{2,x}/(R \cdot T_2), \text{ and the other is } y_{2,T_1} = E_{2,x}/(R \cdot T_1). \text{ There should be a spacing between them. Apparently there is a spacing if I open it with the math editor. Please verify the submitted manuscript.)}$$

Note that, in this case, it is necessary to use the isoconversional activation energy $E_{2,x}$ corresponding to the second curing process. Once $t_{2,iso2}$ is determined, we can calculate the time corresponding to the second curing stage (second heating + second isothermal) as:

$$t_{stage2} = \frac{T_2 - T_1}{\beta_2} + t_{2,iso2} \quad (23)$$

Finally, the total cycle time can be calculated as $t_{cycle} = t_{stage1} + t_{stage2}$.

4 Results and discussion

4.1 Preliminary analysis

Fig. 1 compares the dynamic curing at 10 °C/min of a fresh dual formulation DGJEF_0.5_BG4 and formulations DGJEF_0.5 (without added initiator, equivalent to the first curing process) and DGJEF_0.5_BG4 after precuring at 90 °C for 240 min (equivalent to the second curing process). It can be clearly observed that the first curing process of the dual formulation is hardly affected by the presence of BG. In the absence of BG, the homopolymerization of excess epoxy groups does not take place given the poor nucleophilicity of the aliphatic tertiary amines formed in the epoxy-amine reaction (see Scheme 2), as observed for analogous curing systems [33]. It can also be observed that, after precuring of the dual formulation, the second curing process takes place entirely in the dynamic scan, that is, without premature activation and reaction during the precuring step, at higher temperatures. The heat evolved during the first and second curing process, measured at convenient isothermal temperatures, allowed us to determine that the contribution of each curing process was about 50% of the total [4], as expected from the composition of the formulation (see Table 1). The analysis of the intermediate and final T_g s of different intermediate compositions [4] also indicated that the contribution of each curing process was the expected taking into account the amine-epoxy ratio and the excess of epoxy groups.

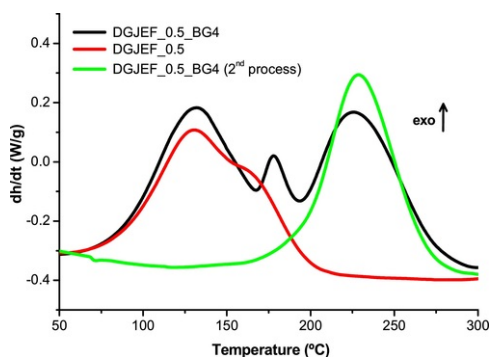
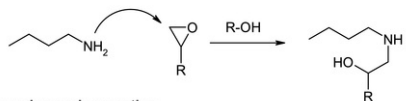


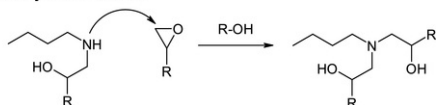
Fig. 1 Comparison of the heat flow curves (dh/dt) corresponding to the dynamic curing at 10 °C/min of the formulations DGJEF_0.5_BG4 (global and 2nd process after pre-curing at 90 °C for 240 min) and DGJEF_0.5 (equivalent to 1st process), adapted from previously reported data [4].

alt-text: Fig. 1

a. Primary amine reaction



b. Secondary amine reaction



Scheme 2 : Epoxy-amine reaction.

alt-text: Scheme 2

Although the curing process can take place in an apparently sequential way [4], Fig. 1 shows that, in the global curing process, there might be some overlapping between the first and second curing process at the prescribed heating rate. This implies that the kinetics analysis of the global curing process, making use of dynamic data [3], may not be feasible. Moreover, the methodology employed by Sun et al. [11], based on the analysis of dynamic curing experiments corresponding to each reaction step, may not be feasible either.

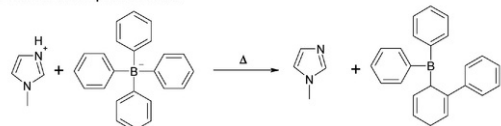
In Fig. 1 it is also noticeable a small peak in the first and second curing process that could be attributed to the activation of the second curing process [4], although this is observed only as a small onset in the dynamic

scan corresponding to the second curing process, after pre-curing at 90 °C for 240 min. These results suggest that the first and second curing process may be somewhat independent from each other, but there are some factors conferring them certain dependence.

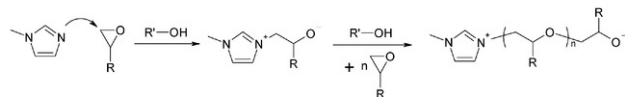
In order to elucidate this, the curing mechanism should be analyzed. A simplified reaction mechanism is shown in [Scheme 2](#). The first reaction is a nucleophilic addition of the primary amine to the epoxy ring, producing a secondary amine and a hydroxyl group ([Scheme 2.a](#)). This is followed by the nucleophilic addition of the secondary amine to the epoxy ring, producing a tertiary amine and another hydroxyl group ([Scheme 2.b](#)). The generated hydroxyl groups confer the epoxy-amine reaction an autocatalytic character, usually caused by the activation of the epoxy ring by proton donors or other activating species [34], although in reality the reaction mechanism is more complex and involves the formation a number of reactive and non-reactive complexes [34-37].

The second curing process is shown in [Scheme 3](#). For the sake of simplicity, a detailed reaction mechanism [3,38,39] is not shown. Given that the aliphatic tertiary amines formed by the epoxy-amine reaction have very poor nucleophilicity, an initiator is necessary to start the anionic homopolymerization of the excess epoxy groups. In the present case there should be, in the first place, the thermal activation of BG, leading to the release of the initiating species, 1-methylimidazole (1MI). This is illustrated in [Scheme 3.a](#) (note that the structure of the boron derivative resulting from the thermal decomposition of BG has been adapted from a non-thermal activating mechanism [17]). The decomposition kinetics of BG leading to 1MI might not depend on the completion of the epoxy-amine reaction, although an effect of the changing chemical environment caused by the epoxy-amine reaction cannot be disregarded at all. [Fig. 2](#) shows that the reaction onset of the second curing process of DGJEF_0.5_BG4 formulation and the neat epoxy formulation DG_BG4 takes place within the same temperature ranges, although the profile of the initiation step, associated with the thermal decomposition of BG [4], is not identical. However, the following reaction steps, especially the initiation and propagation reactions ([Scheme 3.b](#)), are strongly affected by the presence of proton donors such as hydroxyl groups [38], as in the epoxy-amine reaction. Therefore, the reaction kinetics of the second curing stage do depend on the state of completion of the first curing stage, that is, the presence of hydroxyl groups formed as a consequence of the epoxy-amine reaction ([Scheme 2](#)). This is also evidenced in [Fig. 2](#), which shows that the second curing process of DGJEF_0.5_BG4 formulation takes place at lower temperatures than the curing process of the epoxy formulation DG_BG4.

a. Thermal decomposition of BG



b. Anionic epoxy homopolymerization



Scheme 3 : Thermal decomposition of BG (a) and anionic epoxy homopolymerization (b).The structure after the thermal decomposition of the initiator has been adapted from a non-thermal activating mechanism [17].

alt-text: Scheme 3

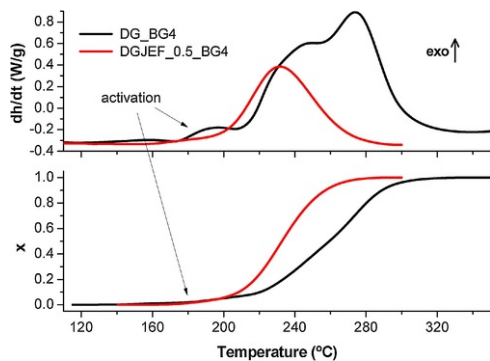


Fig. 2 Comparison of the heat flow (dh/dt) and conversion (x) curves corresponding to the dynamic curing at 10 °C/min of the formulations DG_BG4 and DGJEF_0.5_BG4 (2nd process after pre-curing at 90 °C for 240 min).

alt-text: Fig. 2

Therefore, in the kinetics analysis of the curing process we will take into account that the activation of the second curing reaction is independent from the first curing process. In reality, according to the methodology explained in section 3.1, the whole of the second curing process is regarded as independent from the first curing process, but in reality this is not strictly true. However, this hypothesis will be valid as long as the second curing process (or the majority of it) takes place once the first curing process is over.

4.2 Kinetics analysis

Fig. 3 shows the conversion and rate curves corresponding to the first curing process of DGJEF_0.5_BG4 at different temperatures. The evolution of conversion and rate curves with temperature follows the expected trends. In none of the cases it was observed further reaction beyond the stabilization of the isothermal baseline at the end of the first curing process. The rate curves have an autocatalytic character, as expected for epoxy-amine curing. The reaction heat measured agreed well with the reaction heat reported previously [4].

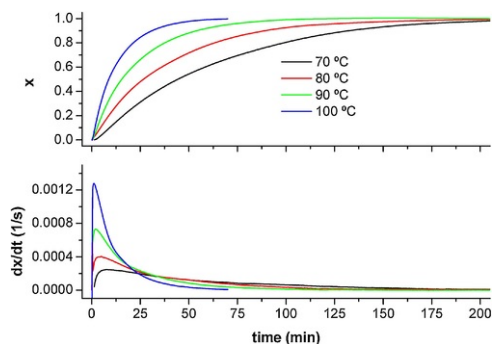


Fig. 3 Conversion x and rate dx/dt for the 1st curing process of DGJEF_0.5_BG4 at different temperatures.

alt-text: Fig. 3

Fig. 4 shows the conversion and rate curves corresponding to the second curing process of DGJEF_0.5_BG4 at different temperatures, after precuring of the samples at 90 °C for 240 minutes. If one compares Fig. 3 and Fig. 4, taking into account the different temperatures employed for the analysis of the first and second curing stages, it is evidenced the significant difference in reaction rate between both curing stages. It can also be observed in Fig. 4 that the rate curves show a small and sharp exotherm at the beginning, which can be associated to the thermal decomposition of the initiator [4], as observed in Fig. 2. After this sharp exotherm, the reaction rate decreases significantly and afterwards it has a noticeable autocatalytic character. One might be tempted to ascribe this to the occurrence of initiator regeneration, leading to an increasing amount of catalytic hydroxyl groups [38], but the initial concentration of hydroxyl groups is already high (due to the preceding epoxy-amine reaction). Rather, it might be a consequence of the chemical environment, more specifically of the polyether structure of the Jeffamine. It is known that polyether structures form unreactive complexes that decrease the reaction rate in the epoxy-amine reaction [37]. A similar phenomenon might occur in this case, producing an important decelerating effect on the initial reaction steps, that is, those involving the nucleophilic addition of 1MI to the epoxy ring. It might also be an influence of the presence of fragments of boron derivatives.

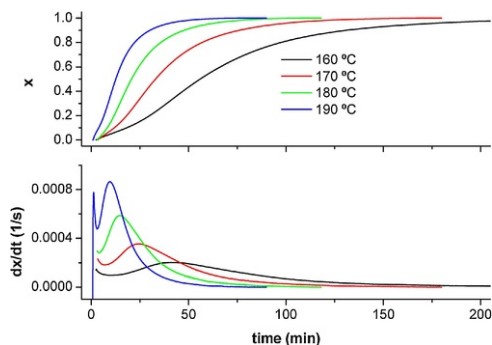


Fig. 4 Conversion x and rate dx/dt for the 2nd curing process at different temperatures, after pre-curing at 90 °C for 240 min.

alt-text: Fig. 4

The results of the application of the isoconversional integral analysis on both the first and second curing processes are shown in Fig. 5. The upper graph shows the values of the integral isoconversional energy throughout the first and second curing process. The error bars reflect the significant uncertainty in the determination of the kinetic parameters in some cases, at the end of the first curing process and, especially, at the beginning of the second curing process. Fig. 4 shows that the determination of the beginning of the second curing process is an important source of error, due to the sharp activation of the latent base, producing some overlapping in the conversion curves up to a degree of conversion of 0.05-0.10.

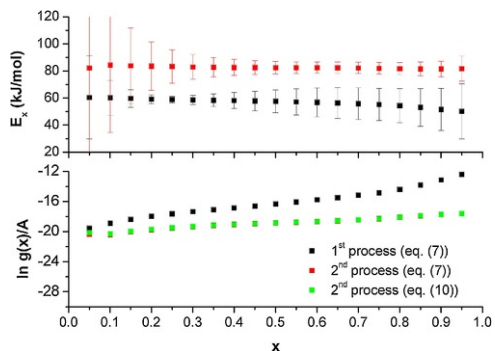


Fig. 5 Results of the isoconversional analysis of the 1st and 2nd curing processes. The error bars indicate the 95% confidence interval for the calculation of E_a from linear regression. A similar relative error was obtained for the intercept at the origin (error bars not shown for clarity purposes).

alt-text: Fig. 5

Fig. 5 shows that, in the case of the first curing process, the activation energy is fairly constant, between 50 and 60 kJ/mol, with a slightly decreasing trend, as reported for other aliphatic amines [14] or other off-stoichiometric amine-epoxy systems [10]. In the case of the second curing process, the activation energy is also fairly constant, with a value around 85 kJ/mol, which is higher than the values reported for the homopolymerization of excess epoxy groups after the thiol-epoxy reaction [3], but similar to the homopolymerization of excess epoxy groups after epoxy-amine addition [10]. The higher value of apparent activation energy for the second curing process indicates also that the separation between both curing processes is promoted at lower temperatures, while some overlapping between processes might occur at high curing temperatures. Sun et al. [11] also observed two well-defined levels of activation energy for the different stages of the curing process.

The lower graph in Fig. 5 shows the evolution of the factor $\ln(g(x)/A_x)$ for both processes. In the case of the second curing process, it has been done using the original expression for isothermal curing processes, Eq. (7) (neglecting the effect of the precuring at 90 °C for 240 minutes), and using the modified expression that takes into account the preceding thermal history, Eq. (11). The differences are only relevant at the beginning of the second curing process, with shorter reaction times, while they become unnoticeable at higher degrees of conversion or longer curing times, which is logical taking into consideration the difference in reactivity between both curing stages. However, for the sake of consistence, the isoconversional lines of the TTT diagram associated to the second curing process will be calculated using the data determined obtained by means of Eq. (11).

4.3 T_g -x relationship

The $T_g(x)$ of the first and second curing process were determined independently making use of the analysis of the initial, intermediate and final materials and making use of the Eq. (13), following the work of Venditti and Gillham [27]. The parameters coming from the analysis are shown in Table 2, along with the parameters λ for both curing processes. The high value of λ_1 (very close to 1) indicate that there is very little crosslinking taking place in the first curing stage, which is consistent with the fact that the conversion at gelation for this formulation is $x_{gel} = 0.45$ [4] or, what is the same, $x_{1,gel} = 0.9$, towards the end of the first curing process. Fig. 6 shows that the experimental determination of the $T_g(x)$ of the first curing process agrees well with the theoretical prediction using Eq. (13), and that the increase in T_g with x is fairly linear. According to Hale et al. [29], the change in glass transition should be linear with respect to conversion before gelation takes place, because the change in T_g is mainly associated with a decrease in free volume of the system. When mobility restrictions caused by crosslinking take place, the $T_g(x)$ should experience a curvature with faster increase in T_g towards the end of the curing process [29]. In contrast, in the second curing stage the value of λ_2 is lower, about 0.6, because crosslinking takes place, almost entirely in the second curing stage, in fact.

Table 2 Parameters for the determination of the $T_g(x)$ relationship of DGJEF_0.5_BG4 formulation using theoretical expression Eq. (13).

alt-text: Table 2

	$T_g (^{\circ}C)$	$\Delta C_p (kJ/kg \cdot K)$
Uncured material (0)	-31	0.512
Intermediate material (int)	23	0.485
Final material (∞)	89	0.300
$T_g(x)$ parameters	$\lambda_1 = 0.947$ $\lambda_2 = 0.619$ $\lambda_{global} = 0.587$	

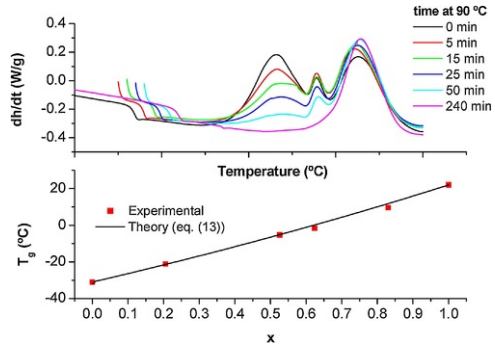


Fig. 6 Experimental determination of the $T_g(x)$ relationship for the 1st curing process of DGJEF_0.5_BG4 formulation and comparison with theoretical predictions (Eq. (13)).

alt-text: Fig. 6

Both $T_g(x)$ relationships have been represented in Fig. 7, but with respect to x_{epoxy} instead of the relative conversion of each curing process. As explained before, we have assumed that, for the first curing process, $x_{epoxy} = 0.5 \cdot x_1$ and that, for the second curing process, $x_{epoxy} = 0.5 + 0.5 \cdot x_2$. It turns out that x_{epoxy} is also equivalent to the global calorimetric conversion, so that we have represented a global $T_g(x)$ relationship taking as reference the uncured and fully cured states, and the parameter λ_{global} in Table 2. The combination of the individual $T_g(x)$ relationships of the first and second curing stages can reproduce correctly the experimentally observed evolution. However, such global relationship is unable to reproduce correctly the experimental points, because the first and second curing stages have different structure and network build-up processes. Note that, in fact, in the definition of Eq. (13) [27] it is assumed that, at any degree of conversion, the system can be described as a mixture of uncured and cured material, but this is only possible if there is a single curing process. Therefore, in dual curing processes, one should define a $T_g(x)$ relationship for each one of the curing processes. One might determine a λ_{global} by numerical adjustment of experimental points, but then the value of this parameter would probably lose its meaning in terms of network build-up. Therefore, we choose to use the combination of the individual relationships in order to properly describe vitrification.

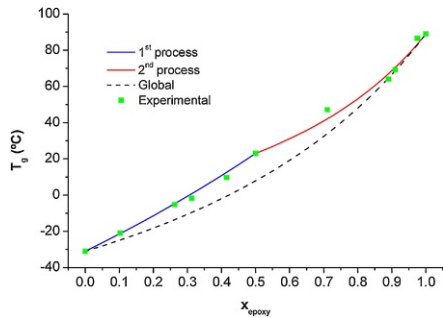


Fig. 7 $T_g(x)$ relationships for the curing process of DGJEF_0.5_BG4 formulation determined experimentally and theoretically.

alt-text: Fig. 7

4.4 Time-temperature-transformation (TTT) diagram

Prior to the TTT diagram, we first present the CTT diagram of the dual-curing process of formulation DGJEF_0.5_BG4. The diagram is simpler, as explained above. It requires mainly the representation of the vitrification line $T_g(x)$ and gelation line x_{gel} . The representation of these two lines allow the identification, around their crossover, of the most relevant states during a curing process, as seen in Fig. 8. In order to verify the quality of the kinetics analysis and the application of the kinetics data to the simulation of other curing schedules, we decided to simulate the whole curing process at 10 °C/min and compare it with the experimental results of the dynamic curing (see Fig. 1). The dynamic curing of both stages was simulated independently following the methodology described in Section 3.4, and then the relative conversions x_1 and x_2 were converted to x_{epoxy} . We integrated the dynamic curing curve at 10 °C/min from Fig. 1 and represented it in the CTT diagram as well. Taking into account the uncertainty in the determination of the baseline for the integration of the global rate curve and other sources of experimental error (note the significant uncertainty in the isoconversional parameters at the end of the first curing process and the beginning of the second curing process, see Fig. 5), the agreement between the predicted and the real data is remarkable, validating the methodology employed. It cannot be ruled out, however, some complex interplay between curing processes, as discussed in Section 4.1, leading to some divergences. This diagram also suggests that the global curing might have been studied using dynamic data, virtually unaffected by vitrification, but the apparently poor separation between curing stages (see Fig. 1) prompted us to use a different methodology.

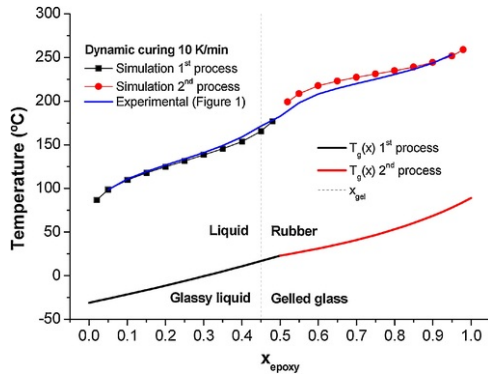


Fig. 8 CTT diagram of the DGJEF_0.5_BG4 formulation. The different states are identified around the crossover between the vitrification ($T_g(x)$) and gelation (x_{gel}) lines. The simulated curing at 10 °C/min is compared with the experimental curing (from the data in Fig. 1).

alt-text: Fig. 8

Fig. 9 plots the TTT diagram corresponding to the curing of the DGJEF_0.5_BG4 formulation. The isoconversional lines have been related to the global epoxy conversion x_{epoxy} (for the first curing process, $x_{epoxy} = 0.5 \cdot x_1$ and that, for the second curing process, $x_{epoxy} = 0.5 + 0.5 \cdot x_2$), rather than the individual conversions. However, the first and second curing processes can be clearly identified because of their radically different kinetics. Note that plotting of the isoconversional lines implies a significant extrapolation beyond the experimental range of the kinetics analysis, but the predicted trends are in agreement with the values of activation energy that were determined from the kinetics analysis (see Fig. 5). The isoconversional curves of the first and second curing process tend to diverge at lower temperatures, while they tend to approach at higher temperatures, because the apparent activation energy of the second curing process is higher than that of the first one. The isoconversional line at gelation was determined according to the gel point determined experimentally and reported in our previous work [4].

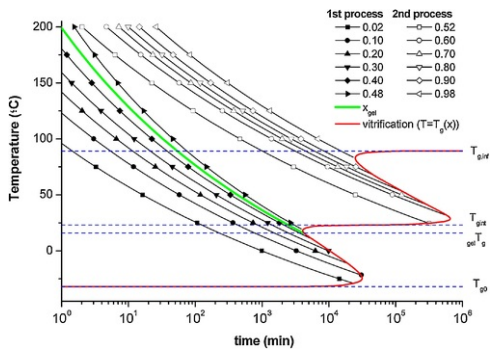


Fig. 9 TTT diagram of the DGJEF_0.5_BG4 formulation. Isoconversional lines are related to x_{epoxy} .

alt-text: Fig. 9

The vitrification line has a shape that is radically different from that of any TTT diagram previously reported in the literature [13-16]. In fact, in addition to T_{g0} , $T_{g\infty}$ and $_{gel}T_g$, one has to include also the intermediate $T_{g,int}$ as a characteristic temperature of the curing process. Instead of the traditional S-shaped vitrification line, there are two overlapping S-shaped curves joining at $T_{g,int}$ that reflect the existence of two curing stages with different $T_g(x)$ relationships and curing kinetics. However, the states that one can find or identify in the TTT diagram (liquid, glassy liquid, rubber, gelled glass) do not change. For the sake of clarity, the identification of the different states has not been included in Fig. 9. The isoconversional lines of the first and second curing processes logically end in the vitrification line corresponding to the respective $T_g(x)$ relationship.

Upon examination of the TTT diagram, one can also validate the hypothesis that the effect of vitrification should not be taken into account in the kinetics analysis. With regards to the first curing process, vitrification would only have been observed if the curing process had been performed below room temperature. That situation is not at all realistic and, in addition, it would have meant an experimental determination within the range of tenths or hundreds of hours. However, with regards to the first curing process, the TTT diagram indicates that the formulation can be stored safely in a fridge (ca. 5 °C) or a freezer (ca. -18 °C) for long periods of time without the risk of gelation. With respect to vitrification in the second curing state, the same considerations can be made, but with even longer time scales because of the slower reaction kinetics.

An interesting remark should be made concerning the storage stability of the intermediate material. In our previous work [4], we reported that intermediate materials were stable for at least 7 weeks, which is about 70000 minutes. Although the isoconversional lines corresponding to the very end of the first curing process (i.e. $x_{epoxy} = 0.499$) and the onset of the second curing process (i.e. $x_{epoxy} = 0.501$) were not plotted, the difference between the isoconversional lines $x_{epoxy} = 0.48$ and $x_{epoxy} = 0.52$ at 30 °C is in the range of 10^5 . In spite of the uncertainty in the kinetic parameters at the end of the first curing process and the beginning of the second curing process (see Fig. 5), the estimation of the isothermal stability at 30 °C is not that far from our experimental stability measurements [4].

Regarding the independence of the curing processes, this would be true for almost any practical curing temperature. Overlapping would only take place at very high curing temperatures, above 180-200 °C or in processes at certain heating rates, as suggested by Fig. 1. In practice, curing processes are commonly carried out in steps at different temperatures, so that a sequential process combining independent curing stages would be guaranteed as long as the first curing process was carried out at a moderate temperature of up to 120 °C-150 °C, providing the exothermicity of the reaction would not produce a temperature runaway. The second curing stage would obviously take place at higher temperatures in order to ensure complete cure in a reasonable time.

A remarkable application of the TTT diagram is the estimation of curing schedules for the processing of thermosets. A first interesting scenario is the calculation of the total cycle time, t_{cycle} , for a two-stage process combining two consecutive isothermal steps. This can be done easily following the methodology described in section 3.4. For instance, for a curing schedule consisting in a first isothermal step at 120 °C followed by a second isothermal step at 180 °C. Let's assume that the duration of the first curing step is $t_{stage1} = 30 \text{ min}$ (note that the time to reach $x_{epoxy} = 0.48$ is 20 minutes, from the TTT diagram), so that we are interested in calculating the time required t_2 at 180 °C to reach $x_{epoxy} = 0.98$. We first calculate $I_1 = \exp(-E_{2,x}/R \cdot T_1) \cdot t_{stage1}$, with E_2 equal to the activation energy at $x_{epoxy} = 0.98$ (corresponding to $x_2 = 0.96$), $T_1 = 120 \text{ °C}$ and $t_1 = 30 \text{ min}$. Then, making use of Eq. (11), we determine $t_{stage2} = 64 \text{ min}$. In consequence, the total reaction time is $t_{cycle} = t_{stage1} + t_{stage2} = 94 \text{ min}$. However, if we read directly the value of t_{stage2} from the isoconversional line $x_{epoxy} = 0.98$ from the TTT diagram (or neglecting the value of I_1), we estimate a value of $t_{stage2} = 65 \text{ min}$. The influence of the precuring time on the curing kinetics of the second stage may be negligible in agreement with the results shown in Fig. 5. In fact, this is caused by the large difference in curing kinetics between the first and second curing stages.

However, if we reconsider the calculation of t_{cycle} taking into consideration the heating ramps and their contribution to the time/temperature integral, the calculation is less straightforward. Let's consider a curing schedule in which the material is first heated from $T_0 = 25\text{ }^{\circ}\text{C}$ to $T_1 = 120\text{ }^{\circ}\text{C}$ with a heating rate $\beta_1 = 10\text{ }^{\circ}\text{C}/\text{min}$, and the material is kept at T_1 until reaching a degree of cure $x_{epoxy} = 0.48$ (close to the end of the first curing process). Then, the material is heated from $T_1 = 120\text{ }^{\circ}\text{C}$ to $T_2 = 180\text{ }^{\circ}\text{C}$ with a heating rate $\beta_2 = 10\text{ }^{\circ}\text{C}/\text{min}$, and the material is kept at T_2 until reaching a degree of cure $x_{epoxy} = 0.98$ (close to the end of the second curing process). The time required in the heating ramps is easy to determine, but the time needed to complete both isothermal steps, $t_{1,iso1}$ and $t_{2,iso2}$, needs to be calculated using eqs. (16) and (19) (and additional expressions). For the first curing stage one can determine $t_{1,iso1} = 18.1\text{ min}$ and $t_{stage1} = 27.6\text{ min}$. For the second curing stage, one can determine $t_{2,iso2} = 60.8\text{ min}$ and $t_{stage2} = 66.8\text{ min}$. The total cycle time is $t_{cycle} = t_{stage1} + t_{stage2} = 94.4\text{ min}$. If one estimated $t_{1,iso1}$ and $t_{2,iso2}$ directly from the TTT diagram (neglecting the contribution of the previous steps to the time/temperature integral), one would have obtained $t_{1,iso1} = 20.4\text{ min}$ and $t_{2,iso2} = 65.2\text{ min}$. This would lead to a total cycle time $t_{cycle} = 101.1\text{ min}$. This is an overestimation of the total cycle time caused by the fact that the curing of both first and second stages does start in the heating ramps. This approximation, taken from the data in the TTT diagram would still produce a reasonable and safe curing schedule, ensuring that the curing reaches an even higher conversion at the end. If one wanted, for example, to estimate the cycle time for partial cure in between stages, directly from the TTT diagram, that would not be a problem either because of the large stability gap between stages. However, the relative error would be higher if one wanted to stop the reaction in the middle of the first or second curing stages, and in that case an exact calculation should be performed instead.

To conclude, the elaboration of the TTT diagram helps us to illustrate the particular behaviour of this dual-curing formulation with latent second stage reactivity. To the best of our knowledge, the behaviour of dual-curing processes had never before been illustrated, in such a clear way, in a TTT diagram. Safe processing and storage conditions can be easily defined. Given the excellent separation between curing stages, these materials are expected to find application in multiple-stage scenarios such as the preparation of highly stable prepregs with controlled properties and reactivity or B-stageable adhesives [4] among others. The main drawback of these materials is their low T_g , which is caused by the highly flexible structure of the Jeffamine diamine crosslinker. In the case of the epoxy homopolymerization, the use of high amount of initiator leads usually to a lower values of T_g [40,41] in comparison with small amounts of initiator [39]. In the present case, the real amount of catalyst is quite low, but the aromatic borate fragments resulting from the initiator decomposition might be causing a certain plasticizing effect, hence explaining the low value of T_g reported [4]. Reducing the amount of initiator for the second curing stage would have a beneficial effect on both the intermediate stability and an increase in T_g . Other aliphatic amines, highly reactive and leading to more rigid network structures, could be used [14,33].

5 Conclusions

The curing kinetics and vitrification behaviour of a dual-curing off-stoichiometric amine-epoxy has been studied, and the results have been used to build a time-temperature-transformation (TTT) that has some unique features in comparison with conventional curing systems, because of the particular characteristics of this dual-curing system.

The results of the kinetics analysis evidence the different reactivity of the first and second curing processes, suggesting that separation and control of the curing sequence is better at lower temperatures. Because these curing processes have different molecular and structure build-up characteristics, vitrification during curing needs to be defined by two different glass transition-conversion relationships.

The TTT diagram summarizes, in a graphical and concise way, the main features of this particular dual-curing system. The latency of the intermediate material at room temperature is made evident, in agreement with previous experimental determinations, and it is easy to find temperature conditions that make it possible to control the curing sequence leading to, in practice, almost independent reaction processes. The TTT diagram also shows a vitrification line that reflects the different network build-up characteristics and kinetics of both curing processes, producing two S-shaped curve joining at the glass transition temperature of the intermediate material. This is the first time this particular behaviour is so clearly shown and illustrated thanks to the TTT diagram.

Acknowledgements

The authors would like to thank MINECO (Ministerio de Economía, Industria y Competividad) (MAT2017-82849-C2-1-R and MAT2017-82849-C2-2-R) and Generalitat de Catalunya (2017-SGR-77 and Serra Hünter programme) for the financial support.

References

- [1] X. Ramis, X. Fernández-Francos, S. De La Flor, F. Ferrando and À. Serra, Click-based dual-curing thermosets and their applications, In: Q. Guo, (Ed), *Thermosets 2nd eEdition: Structure, Properties and Application*, 2017, Elsevier.
- [2] O. Konuray, X. Fernández-Francos, X. Ramis and À. Serra, State of the art in dual-curing acrylate systems, *Polymers* **10**, 2018.

- [3] X. Fernandez-Francos, A.-O. Konuray, A. Belmonte, S. De la Flor, A. Serra and X. Ramis, Sequential curing of off-stoichiometric thiol-epoxy thermosets with custom-tailored structure, *Polymer Chemistry, Chem* **7**, 2016, 2280-2290.
- [4] A.O. Konuray, N. Areny, J.M. Morancho, X. Fernández-Francos, À. Serra and X. Ramis, Preparation and characterization of dual-curable off-stoichiometric amine-epoxy thermosets with latent reactivity, *Polymer* **146**, 2018 42-52.
- [5] D.P. Nair, N.B. Cramer, J.C. Gaipa, M.K. McBride, E.M. Matherly, R.R. McLeod, R. Shandas and C.N. Bowman, Two-Stage Reactive Polymer Network Forming Systems, *Advanced Functional Materials*, *stage reactive polymer network forming systems*, *Adv. Funct. Mater* **22**, 2012, 1502-1510.
- [6] A. Belmonte, X. Fernández-Francos, À. Serra and S. De la Flor, Phenomenological characterization of sequential dual-curing of off-stoichiometric thiol-epoxy systems: *Towards applicability*, *Materials & Design*, *towards applicability*, *Mater. & Des.* **113**, 2017, 116-127.
- [7] F. Saharil, F. Forsberg, Y. Liu, P. Bettotti, N. Kumar, F.N. Haraldsson, Wv. derWijngaart and K.B. Gylfason, Dry adhesive bonding of nanoporous inorganic membranes to microfluidic devices using the OSTE(+) dual-cure polymer, *Journal of Micromechanics and Microengineering*, *Micromech. Microeng.* **23**, 2013, 025021.
- [8] H. Matsushima, J. Shin, C.N. Bowman and C.E. Hoyle, Thiol-Isocyanate Acrylate Ternary Networks by Selective Thiol-Click Chemistry, *Journal of Polymer Science Part A: Polymer Chemistry*, *isocyanate-acrylate ternary networks by selective thiol-click chemistry*, *J. Polym. Sci. A Polym. Chem.* **48**, 2010, 3255-3264.
- [9] J.A. Carioscia, J.W. Stansbury and C.N. Bowman, Evaluation and control of thiol-ene/thiol-epoxy hybrid networks, *Polymer* **48**, 2007, 1526-1532.
- [10] J.M. Morancho, X. Ramis, X. Fernández-Francos, J.M. Salla, A.O. Konuray and À. Serra, Curing of Off-Stoichiometric Amine-Epoxy Thermosets, *Journal of Thermal Analysis and Calorimetry*, *off-stoichiometric amine-epoxy thermosets*, *J. Therm. Anal. Calorim.* 2018, <https://doi.org/10.1007/s10973-018-7158-2>.
- [11] H. Sun, Y. Liu, Y. Wang and H. Tan, Curing Behavior of Epoxy Resins in Two-Stage Curing Process by Non-Isothermal Differential Scanning Calorimetry Kinetics Method, *Journal of Applied Polymer Science*, *curing behavior of epoxy resins in Two-stage curing process by non-isothermal differential scanning calorimetry kinetics method*, *J. Appl. Polym. Sci.* **131**, 2014.
- [12] J.P. Pascault, H. Sautereau, J. Verdu and R.J.J. Williams, *Thermosetting Polymers*, 2002, Marcel Dekker; New York, [etc.].
- [13] X. Ramis and J.M. Salla, Time-temperature transformation (TTT) cure diagram of an unsaturated polyester resin,, *Journal of Polymer Science, Part B: Polymer Physics*, *Polym. Sci. Part B: Polym. Phys.* **35**, 1997, 371-388.
- [14] D. Santiago, X. Fernández-Francos, X. Ramis, J.M. Salla and M. Sangermano, Comparative curing kinetics and thermal-mechanical properties of DGEBA thermosets cured with a hyperbranched poly(ethyleneimine) and an aliphatic triamine, *Thermochimica Acta* **526**, 2011, 9-21.
- [15] H. Teil, S.A. Page, V. Michaud and J.A.E. Manson, TTT-cure diagram of an anhydride-cured epoxy system including gelation, vitrification, curing kinetics model, and monitoring of the glass transition temperature, *Journal of Applied Polymer Science*, *Appl. Polym. Sci.* **93**, 2004, 1774-1787.
- [16] M.T. Aronhime and J.K. Gillham, *Time-Temperature-Transformation (TTT) Cure Diagram of Thermosetting Polymeric Systems*, 1986, Springer-Verlag; Berlin, West Ger, 83-113.
- [17] X. Sun, J.P. Gao and Z.Y. Wang, Bicyclic Guanidinium Tetraphenylborate: A Photobase Generator and A Photocatalyst for Living Anionic Ring-Opening Polymerization and Cross-Linking of Polymeric Materials Containing Ester and Hydroxy Groups, *Journal of the American Chemical Society*, *guanidinium tetraphenylborate: a photobase generator and a photocatalyst for living anionic ring-opening polymerization and cross-linking of polymeric materials containing ester and hydroxy groups*, *J. Am. Chem. Soc.* **130**, 2008, 8130-8131.
- [18] T. Rodima, I. Kaljurand, A. Pihl, V. Mäemets, I. Leito and I.A. Koppel, Acid-Base Equilibria in Nonpolar Media. 2.1 Self-Consistent Basicity Scale in THF Solution Ranging from 2-Methoxy-pyridine to EtP1 (pyrr) Phosphazene, *The Journal of Organic Chemistry*, *base equilibria in nonpolar media. 2.1 self-consistent basicity scale in THF solution ranging from 2-methoxy-pyridine to EtP1 (pyrr) phosphazene*, *J. Org. Chem.* **67**, 2002, 1873-1881.
- [19] S. Vyazovkin and N. Sbirrazzuoli, Isoconversional kinetic analysis of thermally stimulated processes in polymers, *Macromolecular Rapid Communications*, *Rapid Commun.* **27**, 2006, 1515-1532.
- [20] S. Vyazovkin, Modification of the Integral Isoconversional Method to Account for Variation in the Activation Energy, *Journal of Computational Chemistry*, *integral isoconversional method to account for variation in the activation*

energy, *J. Comput. Chem.* **22**, 2001, 178-183.

- [21] M.J. Starink, The determination of activation energy from linear heating rate experiments: a comparison of the accuracy of isoconversion methods, *Thermochimica Acta* **404**, 2003, 163-176.
- [22] L.A. Pérez-Maqueda and J.M. Criado, The Accuracy of Senum and Yang's Approximations to the Arrhenius Integral, *Journal of Thermal Analysis and Calorimetry* **60**, 2000, 909-915.
- [23] X. Ramis, J. Salla, A. Cadenato and J. Morancho, Simulation of isothermal cure of a powder coating, *Journal of Thermal Analysis and Calorimetry* **72**, 2003, 707-718.
- [24] S. Vyazovkin, Evaluation of activation energy of thermally stimulated solid-state reactions under arbitrary variation of temperature, *Journal of Computational Chemistry, Comput. Chem.* **18**, 1997, 393-402.
- [25] A.O. Konuray, X. Fernandez-Francos and X. Ramis, Analysis of the reaction mechanism of the thiol-epoxy addition initiated by nucleophilic tertiary amines, *Polymer Chemistry, Chem.* **8**, 2017, 5934-5947.
- [26] A. Perejón, P.E. Sánchez-Jiménez, J.M. Criado and L.A. Pérez-Maqueda, Kinetic Analysis of Complex Solid-State Reactions. A New Deconvolution Procedure, *The Journal of Physical Chemistry* **115**, 2011, 1780-1791.
- [27] R.A. Venditti and J.K. Gillham, Relationship between the glass transition temperature (T_g) and fractional conversion for thermosetting systems, *Journal of Applied Polymer Science, Appl. Polym. Sci.* **64**, 1997, 3-14.
- [28] J.P. Pascault and R.J.J. Williams, Glass transition temperature versus conversion relationships for thermosetting polymers, *Journal of Polymer Science, Part B: Polymer Physics, Polym. Sci. Part B: Polym. Phys.* **28**, 1990, 85-95.
- [29] A. Hale, C.W. Macosko and H.E. Bair, Glass transition temperature as a function of conversion in thermosetting polymers, *Macromolecules* **24**, 1991, 2610-2621.
- [30] G. Wisanrakkit and J.K. Gillham, Glass transition temperature (T_g) as an index of chemical conversion for a high-T_g amine/epoxy systems, *Journal of Applied Polymer Science, Appl. Polym. Sci.* **41**, 1990, 2885-2929.
- [31] A. Belmonte, F. Däbritz, X. Ramis, A. Serra, B. Voit and X. Fernández-Francos, Cure kinetics modeling and thermomechanical properties of cycloaliphatic epoxy-anhydride thermosets modified with hyperstar polymers, *Journal of Polymer Science Part B: Polymer Physics, Polym. Sci. B Polym. Phys.* **52**, 2014, 1227-1242.
- [32] J.L. Bailleul, V. Sobotka, D. Delaunay and Y. Jarny, Inverse algorithm for optimal processing of composite materials, *Composites Part A: Applied Science and Manufacturing, Part A: Appl. Sci. Manuf.* **34**, 2003, 695-708.
- [33] X. Fernández-Francos and X. Ramis, Structural analysis of the curing of epoxy thermosets crosslinked with hyperbranched poly(ethyleneimine)s, *European Polymer Journal, Polym. J.* **70**, 2015, 286-305.
- [34] B.A. Rozenberg, Kinetics, *Thermodynamics and Mechanism of Reactions of Epoxy Oligomers with Amines, Advances in Polymer Science* **75**, 1986, 113-165.
- [35] S. Swier, G. Van Assche and B. Van Mele, Reaction kinetics modeling and thermal properties of epoxy-amines as measured by modulated-temperature DSC. I. Linear step-growth polymerization of DGEBA + aniline, *Journal of Applied Polymer Science, Appl. Polym. Sci.* **91**, 2004, 2798-2813.
- [36] H.J. Flammersheim, Kinetics and mechanism of the epoxide-amine polyaddition, *Thermochimica Acta* **310**, 1998, 153-159.
- [37] S. Swier, G. Van Assche, W. Vuchelen and B. Van Mele, Role of Complex Formation in the Polymerization Kinetics of Modified Epoxy-Amine Systems, *Macromolecules* **38**, 2005, 2281-2288.
- [38] X. Fernandez-Francos, W.D. Cook, A. Serra, X. Ramis, G.G. Liang and J.M. Salla, Crosslinking of mixtures of DGEBA with bislactone initiated by tertiary amines. IV. Effect of hydroxyl groups on initiation and curing kinetics, *Polymer* **51**, 2010, 26-34.
- [39] S.K. Ooi, W.D. Cook, G.P. Simon and C.H. Such, DSC studies of the curing mechanisms and kinetics of DGEBA using imidazole curing agents, *Polymer* **41**, 2000, 3639-3649.
- [40] X. Fernandez-Francos, J.M. Salla, A. Mantecon, A. Serra and X. Ramis, Crosslinking of mixtures of DGEBA with 1,6-dioxaspiro[4.4]nonan-2,7-dione initiated by tertiary amines, *Polymer Degradation and Stability, Degrad. Stab.* **93**, 2008, 760-769.

Highlights

- Kinetics of a dual-curing system has been studied using isoconversional methods.
 - Time-temperature-transformation (TTT) diagram has been elaborated and discussed.
 - Unique features of dual-curing systems (kinetics/network build-up) are highlighted.
 - Safe multiple-stage curing schedules and storage/stability conditions are predicted.
-

Queries and Answers

Query: Your article is registered as a regular item and is being processed for inclusion in a regular issue of the journal. If this is NOT correct and your article belongs to a Special Issue/Collection please contact d.kaliyaperumal@elsevier.com immediately prior to returning your corrections.

Answer: This is correct.

Query: The author names have been tagged as given names and surnames (surnames are highlighted in teal color). Please confirm if they have been identified correctly.

Answer: Yes

Query: Please check the hierarchy of the section headings and correct if necessary.

Answer: Correct

Query: One or more sponsor names and the sponsor country identifier may have been edited to a standard format that enables better searching and identification of your article. Please check and correct if necessary.

Answer: Correct

Query: Please provide page range or volume/issue for Ref. [10].

Answer: Vol 133 (issue 1) pp 519-527